

Ca²⁺ dynamics in the lumen of the endoplasmic reticulum in sensory neurons: direct visualization of Ca²⁺-induced Ca²⁺ release triggered by physiological Ca²⁺ entry

N.Solovyova, N.Veselovsky¹, E.C.Toescu² and A.Verkhatsky³

The University of Manchester, School of Biological Sciences, 1.124 Stopford Building, Oxford Road, Manchester M13 9PT, ²School of Medicine, Birmingham University, Birmingham B15 2TT, UK and ¹Bogomoletz Institute of Physiology, Bogomoletz Str. 4, Kiev-24, The Ukraine

³Corresponding author
e-mail: alex.verkhatsky@man.ac.uk

In cultured rat dorsal root ganglia neurons, we measured membrane currents, using the patch-clamp whole-cell technique, and the concentrations of free Ca²⁺ in the cytosol ([Ca²⁺]_i) and in the lumen of the endoplasmic reticulum (ER) ([Ca²⁺]_L), using high-(Fluo-3) and low-(Mag-Fura-2) affinity Ca²⁺-sensitive fluorescent probes and video imaging. Resting [Ca²⁺]_L concentration varied between 60 and 270 μM. Activation of ryanodine receptors by caffeine triggered a rapid fall in [Ca²⁺]_L levels, which amounted to only 40–50% of the resting [Ca²⁺]_L value. Using electrophysiological depolarization, we directly demonstrate the process of Ca²⁺-induced Ca²⁺ release triggered by Ca²⁺ entry through voltage-gated Ca²⁺ channels. The amplitude of Ca²⁺ release from the ER lumen was linearly dependent on I_{Ca}.

Keywords: Ca²⁺-induced Ca²⁺ release/Ca²⁺ signalling/Ca²⁺ stores/endoplasmic reticulum/sensory neurons

Introduction

The endoplasmic reticulum (ER) is an essential intracellular organelle, which also serves as a central intracellular Ca²⁺ store. The ER membrane forms an intracellular excitable medium, which can produce both synchronous Ca²⁺ release and propagating Ca²⁺ waves. The release of Ca²⁺ from the ER store upon stimulation regulates a variety of cellular events and processes, including excitation–concentration coupling in muscle (Niggli, 1999), excitation–secretion coupling and Ca²⁺ oscillations in secretory cells (Maruyama *et al.*, 1993; Thorn *et al.*, 1993), regulation of gene expression (Hardingham, 2001), neuronal plasticity (Frenguelli *et al.*, 1996; Rose and Konnerth, 2001), neurotransmitter release and exocytosis (Zucker, 1996), and fertilization signals in oocytes (Galione *et al.*, 1991). In most instances, the release of Ca²⁺ from the ER follows the generation of a signal at the plasma membrane level: either the G-protein-mediated increase in inositol 1,4,5-trisphosphate production (Berridge, 1993; Petersen *et al.*, 1994) or the entry of Ca²⁺ through several types of Ca²⁺-permeable ionic channels (Verkhatsky and Shmigol, 1996).

These second messengers interact with Ca²⁺ release channels of the ER, triggering Ca²⁺ release from the ER lumen (Bezprozvanny *et al.*, 1991; Berridge, 1993). The Ca²⁺-induced Ca²⁺ release (CICR) is triggered by Ca²⁺ ions entering the cytoplasm via voltage/ligand-operated plasmalemmal Ca²⁺ channels and interacting with Ca²⁺-gated Ca²⁺ channels (ryanodine receptors; RyRs) present in the ER membrane. The CICR is believed to be significantly involved in shaping neuronal [Ca²⁺]_i transients (Friel and Tsien, 1992; Marrion and Adams, 1992; Hua *et al.*, 1993; Usachev *et al.*, 1993; Llano *et al.*, 1994; Kano *et al.*, 1995; Shmigol *et al.*, 1995; Verkhatsky and Shmigol, 1996) and numerous studies propose that CICR is important for neuronal functions including synaptic transmission and plasticity (Alford *et al.*, 1993; Garaschuk *et al.*, 1997; Emptage *et al.*, 1999; Krizaj *et al.*, 1999; Rose and Konnerth, 2001). Although cytoplasmic Ca²⁺ recordings from various types of neurons strongly suggest the existence of CICR in physiological conditions, direct demonstration of Ca²⁺ release activated by Ca²⁺ entry through plasmalemmal Ca²⁺ channels has not been achieved. Such a direct demonstration requires real-time simultaneous monitoring of intraluminal free Ca²⁺ dynamics and transmembrane Ca²⁺ currents.

The technique for real-time visualization of intraluminal Ca²⁺ concentration ([Ca²⁺]_L) at a single cell level has been perfected by several groups working with non-excitabile cells (Tse *et al.*, 1994; Chatton *et al.*, 1995; Hofer and Schulz, 1996; Park *et al.*, 1999, 2000). Direct measurements of [Ca²⁺]_L are achieved by using low-affinity Ca²⁺ dyes trapped within the ER; the cytoplasmic portion of the dye is removed by either permeabilization of plasmalemma or by washing it out through the micropipette under a whole-cell patch-clamp configuration. The latter technique was employed successfully in gonadotropes (Tse *et al.*, 1994), hepatocytes (Chatton *et al.*, 1995) and pancreatic acinar cells (Mogami *et al.*, 1998; Park *et al.*, 1999). Here we extended this method to mammalian sensory neurons to characterize directly [Ca²⁺]_L dynamics upon CICR in response to cell depolarization.

Results

Imaging of the ER

The distribution of the ER within dorsal root ganglia (DRG) neurons was assessed by using fluorescent analogues of ryanodine and thapsigargin (TG) or the ER-Tracker. Figure 1A shows a neuron simultaneously stained with ER-Tracker and green fluorescent ryanodine. The staining by both dyes reveals a similar pattern, indicating that the ER occupies most of the cytoplasm, leaving the nuclear region free of labelling. Imaging with green fluorescent TG, performed separately, has demonstrated essentially the same staining pattern (data not shown).

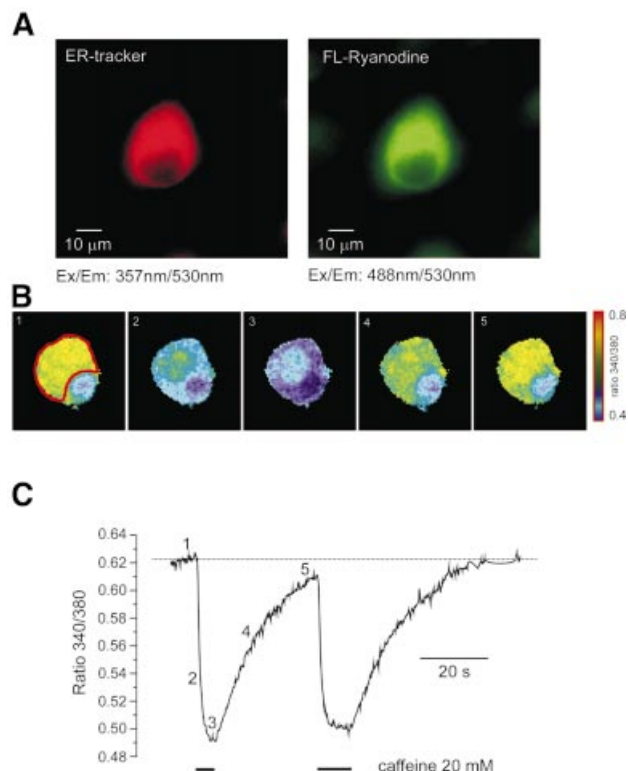


Fig. 1. Imaging of the ER in individual DRG neurons. **(A)** Images of the same DRG neuron stained with ER-Tracker (100 nM, 10 min, left panel) and BODIPY FL-X fluorescent ryanodine (1 μM , 5 min). The fluorescence was excited at 357 (ER-Tracker) and 488 nm (FL-ryanodine) and emitted light was collected at 530 ± 15 nm. **(B)** Imaging of the Ca^{2+} concentration within the ER lumen by Mag-Fura-2. The selected ratio (340/380 nm) images were taken from the DRG neuron after the cytoplasmic portion of the dye was washed out via intracellular dialysis with normal intrapipette solution. The images were taken before, during and after the cell was exposed to 20 mM caffeine. The exact times when images were taken are indicated in **(C)**. **(C)** Caffeine-induced changes in the Mag-Fura-2 ratio taken from the cell shown in **(B)**. Fluorescence was collected from the region of interest (ROI) shown on the first image. Caffeine was applied as indicated on the graph.

Thus, the DRG neurons have an elaborated ER, with a high density of both RyRs and sarco-endoplasmic reticulum Ca^{2+} ATPases (SERCA).

As the next step, we performed functional ER imaging by using a low-affinity Ca^{2+} indicator, Mag-Fura-2. The cells were loaded with the Ca^{2+} probe by incubation with the membrane-permeable form of Mag-Fura-2, so that the probe was trapped both within intracellular organelles and the cytoplasm. To remove the cytoplasmic portion of the dye, we perfused the cells with normal, dye-free, intrapipette solution.

Mag-Fura-2 is a ratiometric Ca^{2+} probe that allows accurate calculation of free Ca^{2+} concentration, which is proportional to the ratio of fluorescent intensities acquired at two different excitation wavelengths, 340 and 380 nm (Grynkiewicz *et al.*, 1985). Hence, the dye present in the cytosol reports low levels of Ca^{2+} concentration, which is manifested by low values of the 340/380 ratio (R). Indeed, the initial R determined at the very beginning of the intracellular perfusion was low, near the R_{\min} levels, indicating that the signal derived predominantly from the

cytosol. During the course of intracellular perfusion, the R value progressively increased until reaching a steady state in 8–10 min after the whole-cell configuration was established. At this stage, the cell images (at 340 and 380 nm and the ratio images) became very similar to those obtained with ER-Tracker and fluorescent ryanodine and/or TG (Figures 1B and 3A). The resting Ca^{2+} concentration determined at this point varied between 60 and 270 μM (average level 177 ± 58 μM , mean \pm SD, $n = 63$). We believe that these values are a reflection of the resting Ca^{2+} concentration within the lumen of the ER.

However, the precision of this $[\text{Ca}^{2+}]_{\text{L}}$ evaluation is not absolute. First, Mag-Fura-2 could have accumulated not only in the ER, but also in other organelles with high levels of free Ca^{2+} ions. Secondly, our calibration procedure was based on measuring the fluorescence of the dye present in intracellular organelles and the cytoplasm, which may interfere with the precise determination of K^* . As the actual K_{D} of the dye may be much higher within the store as compared with the cytoplasm (Golovina and Blaustein, 1997), it is possible that we may in fact underestimate the $[\text{Ca}^{2+}]_{\text{L}}$ values.

With all these reservations, the $[\text{Ca}^{2+}]_{\text{L}}$ value in large DRG neurons varied between 50 and 300 μM , which agrees well with the $[\text{Ca}^{2+}]_{\text{L}}$ levels determined with low-affinity Ca^{2+} probes in other cell types [pancreatic acinar cells, ~ 150 μM (Park *et al.*, 1999); hepatocytes, 630 μM (Chatton *et al.*, 1995); gonadotrophes, 60–200 μM (Tse *et al.*, 1994); fibroblasts, 539 μM (Hofer and Schulz, 1996); and astrocytes, 153 μM (Golovina and Blaustein, 1997, 2000)].

Caffeine-induced $[\text{Ca}^{2+}]_{\text{L}}$ dynamics

As caffeine represents a widely accepted tool for inducing Ca^{2+} release in nerve cells, we investigated its action on $[\text{Ca}^{2+}]_{\text{L}}$ in more detail. For this purpose, we studied the dynamics of $[\text{Ca}^{2+}]_{\text{L}}$ changes in response to caffeine, used at high (20 mM) concentration. At this concentration, caffeine activates RyRs in a Ca^{2+} -independent manner (Sitsapesan and Williams, 1990). Brief (3–10 s) application of 20 mM caffeine in Ca^{2+} -free solution resulted in a rapid decrease of $[\text{Ca}^{2+}]_{\text{L}}$, which remained low as long as caffeine was present in the bath (Figure 1B and C). On washout of the drug, $[\text{Ca}^{2+}]_{\text{L}}$ started to increase back towards the pre-stimulation level.

The amplitude of the caffeine-induced $[\text{Ca}^{2+}]_{\text{L}}$ drop varied between different cells, ranging from 20 to 120 μM . Interestingly, we never observed a complete depletion of the store in response to short caffeine application. On average, caffeine diminished the resting $[\text{Ca}^{2+}]_{\text{L}}$ value by $39 \pm 11\%$ ($n = 41$).

The amplitude of $[\text{Ca}^{2+}]_{\text{L}}$ decrease was directly proportional, in a linear fashion, to the pre-stimulation ('resting') $[\text{Ca}^{2+}]_{\text{L}}$ level: the higher the $[\text{Ca}^{2+}]_{\text{L}}$, the larger the amplitude of $[\text{Ca}^{2+}]_{\text{L}}$ decrease (Figure 2A and B). A similar relationship was observed for the maximal rate of $[\text{Ca}^{2+}]_{\text{L}}$ decrease, which ranged between 6 and 33 $\mu\text{M}/\text{s}$ (Figure 2B). On washout, the $[\text{Ca}^{2+}]_{\text{L}}$ recovered to the resting level, with a half-time recovery constant of 36 ± 9 s (mean \pm SD, $n = 41$).

Finally, we directly compared the changes in luminal and cytoplasmic Ca^{2+} induced by caffeine. In these experiments, $[\text{Ca}^{2+}]_{\text{i}}$ was visualized by use of the low-affinity

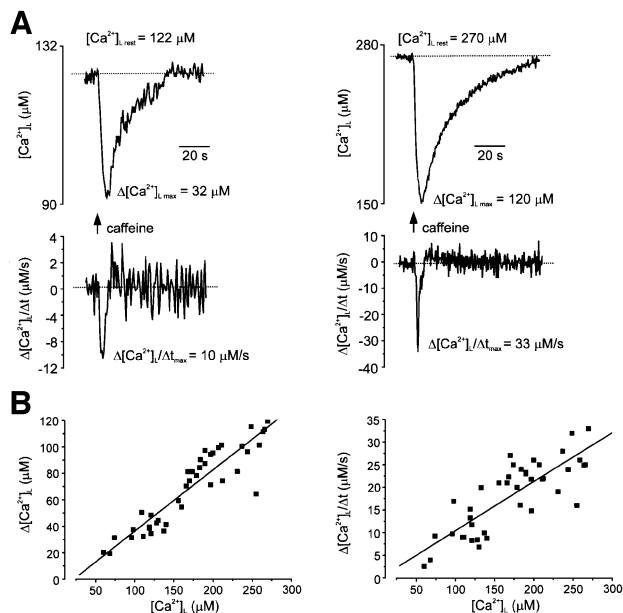


Fig. 2. Caffeine-induced $[Ca^{2+}]_L$ decrease is regulated by the pre-stimulated level of $[Ca^{2+}]_L$. (A) Two examples of caffeine (20 mM)-induced $[Ca^{2+}]_L$ responses obtained from different DRG neurons with different resting $[Ca^{2+}]_L$. Upper traces show calibrated $[Ca^{2+}]_L$ changes whereas their first derivatives are shown at the bottom. The drug was administered for 5 s as indicated on the graph. Note the difference in amplitudes and maximal rate of $[Ca^{2+}]_L$ decrease. (B) Amplitudes ($\Delta[Ca^{2+}]_L$, left panel) and maximal rate of fall of $[Ca^{2+}]_L$ ($\Delta[Ca^{2+}]_L/\Delta t$, right panel) of $[Ca^{2+}]_L$ transients induced by 5 s of 20 mM caffeine applications plotted as a function of resting intraluminal Ca^{2+} concentration. Every point represents an individual cell. The red line shows a linear regression fit.

Ca^{2+} indicator Fluo-3 loaded into the cytoplasm via the patch pipette (see Materials and methods). Application of caffeine triggered co-ordinated changes in $[Ca^{2+}]_i$ and $[Ca^{2+}]_L$, i.e. a drop in ER Ca^{2+} was mirrored by an elevation of $[Ca^{2+}]_i$ (Figure 3).

Ca²⁺ reuptake into the ER store is regulated by $[Ca^{2+}]_L$

The recovery of $[Ca^{2+}]_L$ after the removal of caffeine reflects the SERCA-dependent Ca^{2+} reuptake into the ER lumen as demonstrated by the fact that this recovery could be completely prevented by addition of 5 μM TG immediately after the end of caffeine application ($n = 7$; data not shown).

We also used TG to compare the process of caffeine-induced Ca^{2+} release with another, less specific, Ca^{2+} release process, i.e. the passive Ca^{2+} leakage from the store that is unmasked in the presence of TG, when Ca^{2+} leakage across the ER membrane is not counterbalanced by SERCA pumps (Mogami *et al.*, 1998). The typical experimental protocol employed is shown in Figure 4. First, the cell was stimulated with caffeine for 5 s, which triggered a rapid decrease in $[Ca^{2+}]_L$. After caffeine washout and recovery of the $[Ca^{2+}]_L$ levels, the cell was then exposed to 5 μM of TG. This resulted in a relatively slow $[Ca^{2+}]_L$ decrease that became even slower as the store continued to empty. As the steady-state level was reached, the caffeine/TG-sensitive store was fully depleted, as further application of caffeine failed to release more $[Ca^{2+}]_L$ (Figure 4A). It was notable that TG depleted the

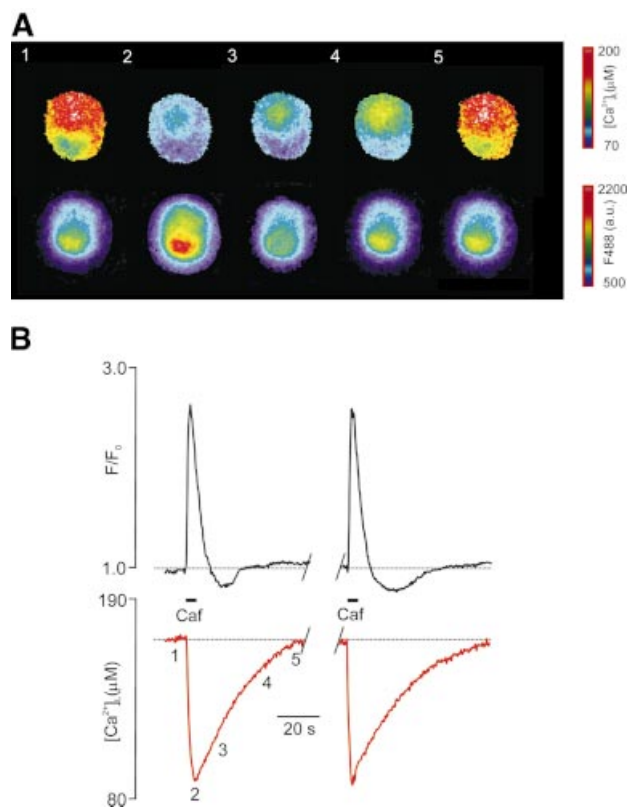


Fig. 3. Simultaneous visualization of $[Ca^{2+}]_i$ and $[Ca^{2+}]_L$ dynamics in DRG neurons. (A) Selected images of the Mag-Fura-2 ratio (340/380 nm, upper panel) taken simultaneously with images of Fluo-3 fluorescent intensity (488 nm) from the DRG neuron exposed to 20 mM caffeine. The ROI for further measurements is drawn over the first image. (B) Calibrated recordings of $[Ca^{2+}]_L$ and normalized Fluo-3 fluorescent intensity (reflecting changes in $[Ca^{2+}]_i$) taken from the cell shown in (A). Caffeine was applied as indicated on the graph; the positions of the images shown in (A) are shown near the $[Ca^{2+}]_L$ trace.

ER to the same extent as caffeine (Figure 4A and B). Moreover, both caffeine and TG decreased $[Ca^{2+}]_L$ rather homogeneously throughout the ER-rich part of the cell (Figure 4A), further indicating the overlap between the caffeine- and TG-sensitive ER compartments.

The residual level of $[Ca^{2+}]_L$ that remained after the stores were discharged either by caffeine or TG most probably represents the free Ca^{2+} remaining in the ER, since application of 5 μM of carbonylcyanide *m*-chlorophenylhydrazone (CCCP) after caffeine or TG did not trigger further changes in $[Ca^{2+}]_L$ ($n = 5$ and 3, respectively; data not shown). Furthermore, application of ionomycin in Ca^{2+} -free solutions following TG brought $[Ca^{2+}]_L$ to zero (R_{min}) level ($n = 5$, Figure 4A, inset).

The experimental protocol described above was used to derive the relationship between the actual $[Ca^{2+}]_L$ and the rates of Ca^{2+} reuptake and Ca^{2+} leakage, as shown in Figure 4C, that were calculated from the trace shown in Figure 4B. The rate of Ca^{2+} uptake, measured after the removal of caffeine, was steeply dependent on $[Ca^{2+}]_L$, being very high when the store was maximally depleted and gradually decreasing as the ER refilled. The rate of Ca^{2+} leakage showed an opposite dependence on $[Ca^{2+}]_L$: it was negligible when the store was depleted and increased before saturating at resting $[Ca^{2+}]_L$.

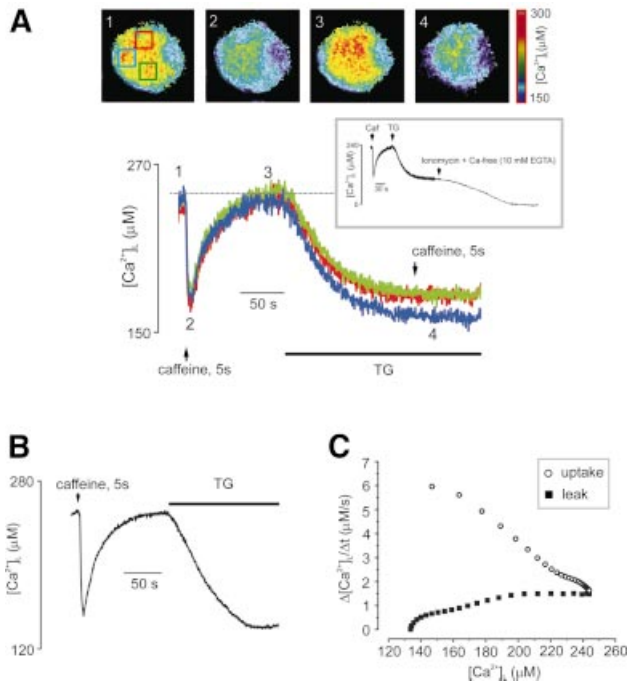


Fig. 4. Ca^{2+} release, Ca^{2+} reuptake and Ca^{2+} leak from the ER store: dependence on $[\text{Ca}^{2+}]_{\text{L}}$. (A) $[\text{Ca}^{2+}]_{\text{L}}$ was measured separately from three ROIs from the neuron, images of which and the ROI positions (distinguished by colours) are shown on the top. The lower panel shows $[\text{Ca}^{2+}]_{\text{L}}$ traces, colour coded according to the respective ROI. Initial application of caffeine triggered rapid Ca^{2+} release followed by $[\text{Ca}^{2+}]_{\text{L}}$ reuptake after removal of agonist. When $[\text{Ca}^{2+}]_{\text{L}}$ recovered to the pre-stimulated level, 5 μM thapsigargin was added to block the SERCA pumps. This resulted in a slow decrease in $[\text{Ca}^{2+}]_{\text{L}}$ due to an unopposed leakage from the store. Note that caffeine and TG reduced $[\text{Ca}^{2+}]_{\text{L}}$ to the same extent. The inset shows that application of ionomycin in Ca^{2+} -free, EGTA-containing solution following TG led to a complete depletion of the store. (B) $[\text{Ca}^{2+}]_{\text{L}}$ trace taken from another DRG neuron employing the protocol described in (A). (C) The relationship between Ca^{2+} transport rates and $[\text{Ca}^{2+}]_{\text{L}}$, derived from the data shown in (B). The uptake rate was leak-corrected.

The maximal rate of uptake was $6 \pm 0.85 \mu\text{M/s}$ (mean \pm SD, $n = 6$; all experiments were performed on neurons with resting $[\text{Ca}^{2+}]_{\text{L}}$ ranging between 230 and 270 μM) and the maximal leak rate was $1.48 \pm 0.17 \mu\text{M/s}$ (mean \pm SD; $n = 6$).

Direct demonstration of CICR in sensory neurons

Most of the experimental support currently available for the existence of physiological CICR (i.e. CICR triggered by Ca^{2+} entry during depolarization) in neurons is based on indirect evidence, originating from measurements of cytoplasmic, not luminal, Ca^{2+} concentration (see for example Friel and Tsien, 1992; Marrion and Adams, 1992; Hua *et al.*, 1993; Usachev *et al.*, 1993; Shmigol *et al.*, 1995; Garaschuk *et al.*, 1997; Hernandez-Cruz *et al.*, 1997). Using the combination of low- and high-affinity probes that independently report Ca^{2+} changes within cytosolic and intra-ER compartments, we were able to address directly the question of whether Ca^{2+} entry through voltage-gated plasmalemmal channels can indeed trigger release of Ca^{2+} from the ER lumen.

For this purpose, we monitored $[\text{Ca}^{2+}]_{\text{i}}$ and $[\text{Ca}^{2+}]_{\text{L}}$ in a voltage-clamped neuron as shown in Figure 5. First, we

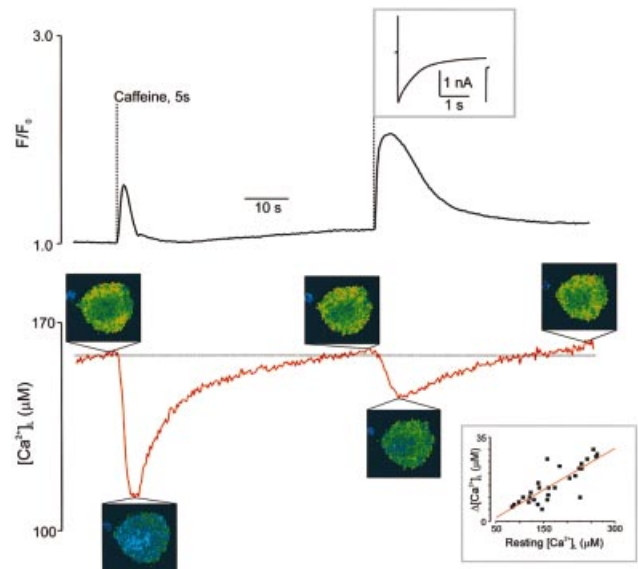


Fig. 5. Direct visualization of Ca^{2+} -induced Ca^{2+} release in DRG neurons. Simultaneous recordings of cytoplasmic Ca^{2+} (normalized Fluo-3 fluorescent intensity, upper trace) and $[\text{Ca}^{2+}]_{\text{L}}$ dynamics recorded from the same neuron are presented. The cell was challenged subsequently by an application of caffeine (20 mM) and by a 3 s step depolarization from -70 to 0 mV (the corresponding Ca^{2+} current is shown in the inset on the top of the Fluo-3 trace). Note that depolarization triggers an increase in cytoplasmic Ca^{2+} and a decrease in $[\text{Ca}^{2+}]_{\text{L}}$. Selected images of the Mag-Fura-2 ratio are shown near the $[\text{Ca}^{2+}]_{\text{L}}$ trace. The inset in the right lower corner shows a linear relationship between resting luminal Ca^{2+} concentration and the amplitude of depolarization-induced $[\text{Ca}^{2+}]_{\text{L}}$ decrease.

probed the ER store with caffeine, which was applied for 5 s. As also shown in Figure 3, this application induced an increase in $[\text{Ca}^{2+}]_{\text{i}}$ and a decrease in the concentration of $[\text{Ca}^{2+}]_{\text{L}}$. After complete recovery of the Ca^{2+} concentration in both compartments, we depolarized the cell from -70 to 0 mV, evoking substantial Ca^{2+} current (I_{Ca}). The depolarization resulted in a significant $[\text{Ca}^{2+}]_{\text{i}}$ elevation as well as a transient decrease in $[\text{Ca}^{2+}]_{\text{L}}$. The amplitude of $[\text{Ca}^{2+}]_{\text{L}}$ decrease was smaller than that evoked by caffeine, ranging between 5 and 30 μM . The amplitude of this depolarization-evoked $[\text{Ca}^{2+}]_{\text{L}}$ drop correlated linearly with the resting $[\text{Ca}^{2+}]_{\text{L}}$: i.e. at higher resting $[\text{Ca}^{2+}]_{\text{L}}$ there was a larger $[\text{Ca}^{2+}]_{\text{L}}$ drop in response to depolarization (Figure 5, inset). When Ca^{2+} current was blocked by Ca^{2+} removal from extracellular solution, both $[\text{Ca}^{2+}]_{\text{i}}$ and $[\text{Ca}^{2+}]_{\text{L}}$ responses disappeared completely ($n = 4$; data not shown). Therefore, these observations demonstrate directly that plasmalemmal Ca^{2+} entry triggers Ca^{2+} release from the ER lumen.

A definite association between the depolarization-evoked decrease in $[\text{Ca}^{2+}]_{\text{L}}$ and the RyRs required further experiments, using established modulators of these receptors. It is known (Sitsapasan and Williams, 1990; Usachev and Thayer, 1997) that at low concentrations (0.5–1 mM), caffeine sensitizes RyRs to cytosolic Ca^{2+} ions. In our experiments, the application of 1 mM caffeine to the DRG neuron, which on its own did not affect $[\text{Ca}^{2+}]_{\text{L}}$ or $[\text{Ca}^{2+}]_{\text{i}}$, significantly increased the amplitude of the $[\text{Ca}^{2+}]_{\text{L}}$ drop in response to the Ca^{2+} current evoked by 3 s depolarization (Figure 6A). This potentiation of Ca^{2+} release occurred despite the fact that the amplitude of I_{Ca}

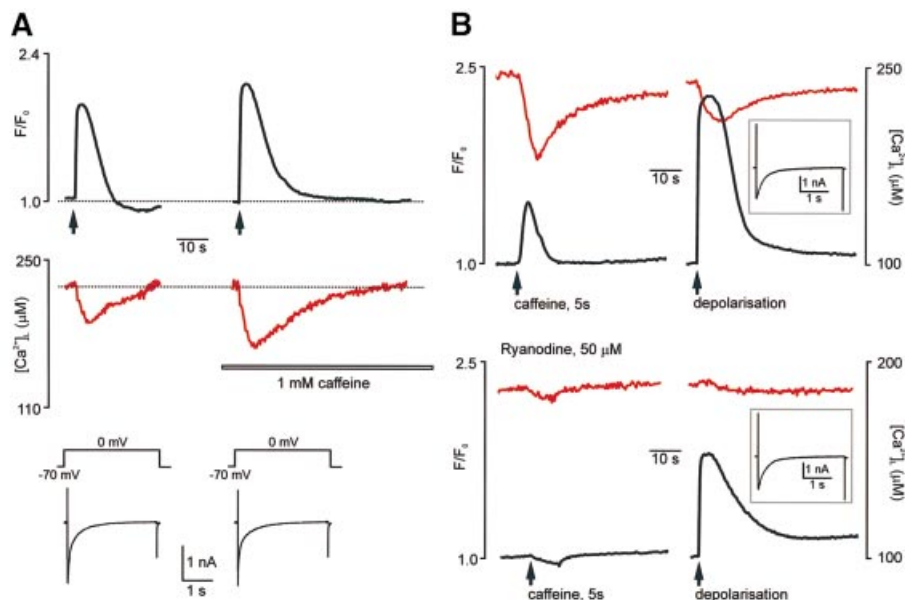


Fig. 6. Pharmacological manipulation with CICR. (A) A low (1 mM) caffeine concentration enhances the CICR. The $[Ca^{2+}]_i$ (black traces) and $[Ca^{2+}]_L$ (red traces) were measured from the same DRG neuron. The neuron was stimulated by 3 s depolarizations in control conditions and in the presence of 1 mM caffeine (the instants of depolarizations are indicated by arrows). Note the significant rise in the amplitude of the $[Ca^{2+}]_L$ decrease in the presence of caffeine. The corresponding Ca^{2+} currents are shown on the lower panel at a higher time resolution. (B) Ryanodine completely inhibits both caffeine- and Ca^{2+} -induced Ca^{2+} release. The upper panel shows control $[Ca^{2+}]_i$ and $[Ca^{2+}]_L$ traces (depicted in black and red, respectively) in response to 20 mM caffeine and 3 s depolarization. The lower panel demonstrates the same experiment performed on another neuron from the same culture after 10 min incubation with 50 μ M ryanodine. Ca^{2+} currents are shown in the insets.

(and hence the amount of Ca^{2+} ions entering the cell) remained unchanged. On average, the amplitude of I_{Ca} -induced $[Ca^{2+}]_L$ decrease was $87 \pm 8\%$ ($n = 7$) larger in the presence of 1 mM of caffeine as compared with the control.

Another test was the use of a specific inhibitor of CICR, ryanodine, which at high concentrations (50–100 μ M) completely inhibits RyRs, and hence blocks the caffeine-induced Ca^{2+} release as well as CICR. In these experiments (Figure 6B), we first measured the caffeine- and depolarization-induced responses of $[Ca^{2+}]_i$ and $[Ca^{2+}]_L$ in control conditions. Then the same coverslip was incubated with 50 μ M ryanodine for 10 min. We found that such a treatment completely blocked caffeine-induced responses of both $[Ca^{2+}]_i$ and $[Ca^{2+}]_L$ in all cells studied ($n = 9$). Ryanodine also completely inhibited CICR, as judged by the absence of $[Ca^{2+}]_L$ changes in response to depolarization ($n = 9$). The Ca^{2+} current as well as depolarization-induced $[Ca^{2+}]_i$ elevation, however, remained.

CICR is directly proportional to the amount of Ca^{2+} entry

Previous investigations of neuronal CICR suggested that significant release through RyRs requires a large Ca^{2+} entry, i.e. CICR became apparent only when a certain threshold of ‘trigger’ Ca^{2+} in the cytosol is reached (Llano *et al.*, 1994; Shmigol *et al.*, 1995). We addressed this question directly, by investigating the relationship between $[Ca^{2+}]_L$ dynamics and Ca^{2+} entry via voltage-gated channels.

First, stimulation of DRG neurons by 3 s depolarizations separated by 20 s intervals triggered almost identical events of Ca^{2+} release from the ER. As shown in Figure 7A, every Ca^{2+} current evoked a drop in $[Ca^{2+}]_L$ with an amplitude of 10–11 μ M. Thus, identical Ca^{2+} entries trigger similar release of Ca^{2+} from the ER lumen.

Different responses occurred when Ca^{2+} entry was graded. First, we stimulated the DRG neurons by a standard I–V protocol, when the cell was depolarized from -70 mV by a series of 400 ms steps with increasing amplitude. This stimulation resulted in a characteristic bell-shaped pattern of $[Ca^{2+}]_i$ transients, which were mirrored by transient $[Ca^{2+}]_L$ decreases (Figure 7B).

A similar relationship was also observed when we graded Ca^{2+} entry by varying the duration of I_{Ca} between 50 and 3000 ms (Figure 8). When stimulating the neurons, we found that the shortest I_{Ca} (50 ms) already induced Ca^{2+} release, as shown by a $[Ca^{2+}]_L$ transient decrease. The increase in the duration of the I_{Ca} resulted in an almost linear increase in the amplitude of Ca^{2+} release (Figure 8A). This linear relationship is illustrated quantitatively in Figure 8C, which plots the amplitude of $[Ca^{2+}]_L$ decrease against the actual charge (Q) carried by the Ca^{2+} current, which directly reflects the number of Ca^{2+} ions entering the cell. From this type of data, we can derive the ‘unitary CICR potency’ of the Ca^{2+} current by dividing the charge carried by a given current by the amplitude of the corresponding $[Ca^{2+}]_L$ transient decrease. This ‘unitary CICR potency’ would thus be a measure of how many pC carried by a Ca^{2+} current are required to release 1 μ M of Ca^{2+} from the store. Figure 8D shows the average

$Q/\Delta[\text{Ca}^{2+}]_{\text{L}}$ values plotted against I_{Ca} duration obtained for five different experiments analogous to that shown on Figure 8A. For these experiments, we have chosen five different cells with similar levels of resting $[\text{Ca}^{2+}]_{\text{L}}$ (range 230–270 μM). The plot shows that the ‘unitary CICR

potency’ of Ca^{2+} current remains constant for currents of different length, thus demonstrating the graded relationship between Ca^{2+} entry and Ca^{2+} release in neuronal cells.

Discussion

CICR in sensory neurons

The existence of ER Ca^{2+} stores in nerve cells with a full complement of Ca^{2+} release channels has been firmly established (for initial observations see Lipscombe *et al.*, 1988; Thayer *et al.*, 1988; Brorson *et al.*, 1991). Nonetheless, the functional dynamics of Ca^{2+} movements between store lumen and cytoplasm upon physiological stimulation of nerve cells remains completely unexplored. The current evidence for a functional CICR (i.e. CICR triggered by Ca^{2+} entry via plasmalemmal Ca^{2+} channels) in neurons is based only on an indirect approach, measuring the cytosolic Ca^{2+} changes, from which it is difficult to distinguish the extra- and intracellular components of the Ca^{2+} transients that follow the activation of the plasmalemmal Ca^{2+} currents. The only attempt at measuring $[\text{Ca}^{2+}]_{\text{L}}$ in neuron-like preparations was performed recently by transfecting PC12 pheochromocytoma cells with ER-targeted aequorin (Alonso *et al.*, 1999). These recordings, however, measured average $[\text{Ca}^{2+}]_{\text{L}}$ changes in the whole culture, and the experimental limitations precluded both I_{Ca} monitoring and cell stimulation in physiologically relevant time frames. By combining Ca^{2+} probes with different affinities and spectral properties, we describe here fluorescence measurements that can differentiate between two distinct intracellular compartments, the ER and the cytoplasm.

Using this direct approach, we show, for the first time, that the dynamics of Ca^{2+} concentration changes within the ER in response to physiological stimulation of single

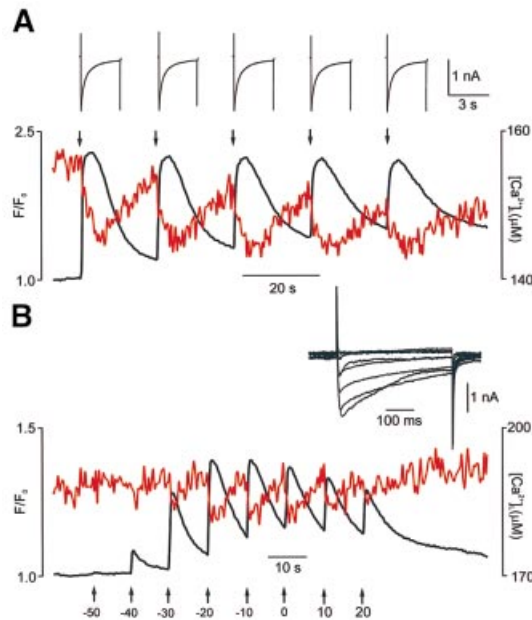


Fig. 7. CICR is graded by Ca^{2+} entry (1). (A) $[\text{Ca}^{2+}]_{\text{L}}$ and $[\text{Ca}^{2+}]_{\text{i}}$ dynamics (red and black traces, respectively) recorded from the DRG neuron stimulated by five consecutive depolarizations (moments of depolarizations are indicated by arrows) from -70 to 0 mV. Ca^{2+} currents are shown above at a higher time resolution. (B) Similarly to the experiment described above, $[\text{Ca}^{2+}]_{\text{L}}$ and $[\text{Ca}^{2+}]_{\text{i}}$ (red and black traces) were recorded in response to step depolarizations of increasing amplitude. Holding potential -70 mV, step increment 10 mV.

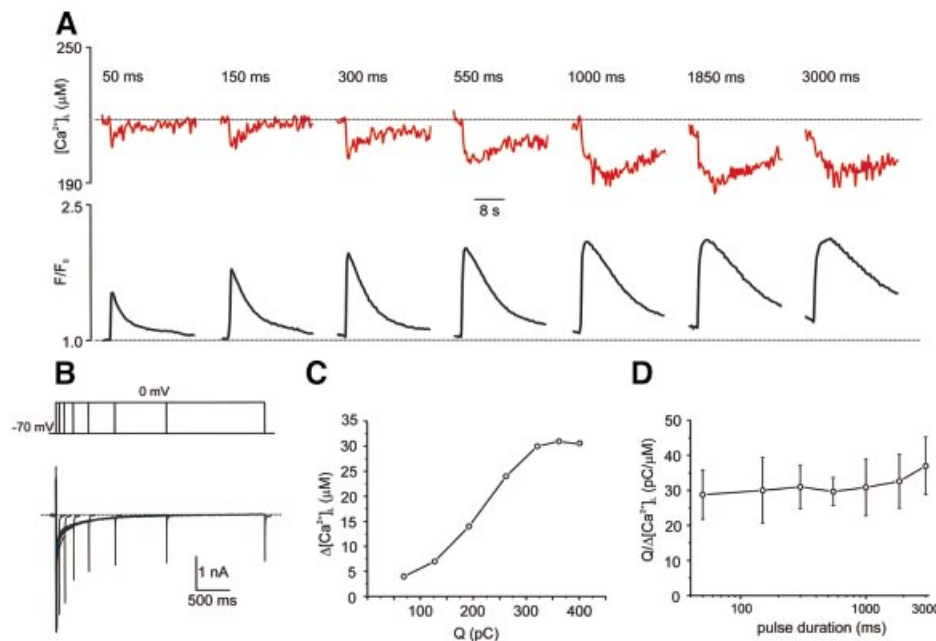


Fig. 8. CICR is graded by Ca^{2+} entry (2). (A) Changes in $[\text{Ca}^{2+}]_{\text{L}}$ (upper panel, red traces) and $[\text{Ca}^{2+}]_{\text{i}}$ (lower panel, black traces) in response to step depolarizations from -70 mV to 0 mV of increasing duration. (B) Voltage protocol and Ca^{2+} currents from the experiment shown in (A). (C) The relationship between the charge carried by the Ca^{2+} current (Q) and the amplitude of the $[\text{Ca}^{2+}]_{\text{L}}$ decrease ($\Delta[\text{Ca}^{2+}]_{\text{L}}$) derived from the traces shown in (A) and (B). (D) The ratio between the charge carried by I_{Ca} and the amplitude of $[\text{Ca}^{2+}]_{\text{L}}$ decrease plotted against duration of corresponding Ca^{2+} currents. Data are mean \pm SD derived from five independent experiments similar to those shown in (A).

neurons. This allowed us to demonstrate clearly that Ca^{2+} entry via voltage-gated Ca^{2+} channels triggers Ca^{2+} loss from the ER, thus proving unequivocally the existence of physiological CICR in nerve cells.

Activation of voltage-gated Ca^{2+} currents following a depolarization pulse resulted in changes in the opposite direction in the fluorescence signals derived from the cytoplasm and the ER lumen; an increase in $[\text{Ca}^{2+}]_i$ was associated with a simultaneous decrease of $[\text{Ca}^{2+}]_L$. This decrease reflects the process of CICR, since the manipulations of the RyRs, which mediate CICR, selectively affected $[\text{Ca}^{2+}]_L$ dynamics in response to I_{Ca} . Thus, sensitization of RyRs by incubation with low (1 mM) concentrations of caffeine increased the CICR amplitude almost 2-fold, although the Ca^{2+} current remained unaffected. Also, blockade of RyRs by 50 μM ryanodine completely inhibited the CICR-related decrease in $[\text{Ca}^{2+}]_L$, again without any apparent effect on Ca^{2+} current parameters.

An important issue in neuronal CICR activation is the relationship between Ca^{2+} entry and the activation of Ca^{2+} release. Most of the previous studies on neuronal CICR showed a non-linear relationship between the amount of Ca^{2+} entry (as measured by the Ca^{2+} current integral) and the corresponding rise in the amplitude of the $[\text{Ca}^{2+}]_i$ transient (Hua *et al.*, 1993, 1994; Llano *et al.*, 1994; Shmigol *et al.*, 1995). These observations suggested a relatively high threshold for CICR activation in neurons as compared with heart muscle cells. For example, in DRG neurons, CICR became apparent (Shmigol *et al.*, 1995) only with an I_{Ca} activation time in excess of 200 ms (compare with 4 ms for cardiac muscle; Han *et al.*, 1994).

Direct monitoring of $[\text{Ca}^{2+}]_L$ changes showed that the degree of CICR activation, as measured by the decrease in $[\text{Ca}^{2+}]_L$, correlated linearly with the amount of Ca^{2+} entering the cytoplasm. This was apparent when Ca^{2+} entry was graded by varying either the amplitude of the depolarization step (Figure 7) or the length of the Ca^{2+} current (Figure 8). Moreover, by calculating the ratio between the charge carried by I_{Ca} and the amplitude of $[\text{Ca}^{2+}]_L$ decrease (Figure 8D), we found that the amount of Ca^{2+} ions required to release 1 μM of Ca^{2+} from the store remained constant for a wide range of I_{Ca} duration. Only at very long I_{Ca} (3 s) did the CICR show a tendency for saturation, presumably reflecting an equilibrium between Ca^{2+} entry into the cytoplasm (from both extra- and intracellular sources) and Ca^{2+} buffering/extrusion, so that no further recruitment of RyRs occurs.

Thus, we conclude that the ER represents an important Ca^{2+} storage organelle in DRG neurons. It occupies most of the cytoplasm and contains a high (>100–200 μM) concentration of free, releasable Ca^{2+} . A proportion of this Ca^{2+} is readily available for Ca^{2+} signals activated by cell depolarization. The CICR in DRG neurons is graded linearly by Ca^{2+} entry and is limited to ~10% of the stored Ca^{2+} .

Luminal Ca^{2+} controls Ca^{2+} release and Ca^{2+} uptake

Release of Ca^{2+} ions from the ER is controlled not only by the changes in cytosolic Ca^{2+} but also by the level of $[\text{Ca}^{2+}]_L$. By analysing the $[\text{Ca}^{2+}]_L$ transients induced by caffeine application in cells that had different levels of $[\text{Ca}^{2+}]_L$, we found that $[\text{Ca}^{2+}]_L$ controls the amplitude and

maximal rate of Ca^{2+} release in a linear fashion. This shows that when all RyRs are activated in the presence of maximal caffeine concentration, Ca^{2+} release is governed by the electrochemical driving force between the ER lumen and cytosol. Similarly, the rate of resting Ca^{2+} leak from the ER depends on $[\text{Ca}^{2+}]_L$, with the leak being maximal when the stores are full.

In addition, the $[\text{Ca}^{2+}]_L$ level controls the refilling of the store after it has been discharged. The rate of Ca^{2+} uptake was maximal when the caffeine/TG stores were maximally depleted. In this respect, DRG neurons show a behaviour similar to that found in non-excitable pancreatic acinar cells (Mogami *et al.*, 1998). The notable difference was that the actual rates of Ca^{2+} uptake/leak were substantially higher in neurons. That is, in pancreatic cells, the maximal rates of leak and uptake were 19 and 95 $\mu\text{M}/\text{min}$, respectively, whereas in neurons they were 90 and 360 $\mu\text{M}/\text{min}$, respectively. This implies a relatively high resting turnover of Ca^{2+} ions across the ER membrane.

Finally, we found that neither caffeine nor TG are able to deplete the neuronal intracellular Ca^{2+} store fully: in both conditions, $[\text{Ca}^{2+}]_L$ remained, even after full agent-dependent depletion, at a relatively high level (~50–60% of the pre-stimulated value). Obviously, this might reflect a limitation of the method, suggesting that part of the signal comes from an intracellular compartment not connected with the caffeine- or TG-sensitive portion of the ER (although not from mitochondria, as CCCP does not affect the degree of store depletion). Alternatively, such a limitation of the release could be an intrinsic property of the store, since a fall in luminal Ca^{2+} content decreases the availability and open probability of RyRs (Lukyanenko *et al.*, 1996; Shmigol *et al.*, 1996). Such a mechanism, which will prevent a severe depletion of the store, may be an important factor in preserving the integrity of the ER (Paschen, 2001; Petersen *et al.*, 2001).

Materials and methods

Simultaneous measurements of Ca^{2+} in the store and in the cytoplasm

DRG neurons were isolated enzymatically from neonatal (1–3 days old) Sprague–Dawley rats using a conventional treatment with 0.1% protease (type XIV) in HEPES-buffered minimum essential Eagle's medium (MEM) for 8 min at 37°C. Individual cells were separated mechanically and plated on poly-L-ornithine- (1 mg/ml) and laminin (0.01 mg/ml)-covered glass coverslips. Neurons were maintained in culture media [Dulbecco's modified Eagle's medium (DMEM), supplemented with 10% horse serum, 50 U/ml penicillin/streptomycin mixture and 6 $\mu\text{g}/\text{ml}$ insulin] at 37°C in an atmosphere of 95% CO_2 + 5% O_2 for 1–2 days prior to the experiment.

For $[\text{Ca}^{2+}]_L$ recordings, we used Mag-Fura-2 (K_D ~25–50 μM) suitable for detecting high intraluminal $[\text{Ca}^{2+}]$ levels (Park *et al.*, 1999). The neurons were incubated with 5 μM Mag-Fura-2 for 30 min at 37°C and washed at 37°C for 1 h prior to the experiment (loading at 37°C promotes dye compartmentalization within the ER lumen; Golovina and Blaustein, 1997; Thomas *et al.*, 2000).

The whole-cell patch-clamp configuration was established on cells loaded with Mag-Fura-2. In the present study, we investigated only large (proprioceptive) neurons with somas >35 μm in diameter. Before establishing the whole-cell configuration, Mag-Fura-2 was evenly distributed between organelles and the cytosol, as judged by fluorescence imaging. Immediately after establishing the whole-cell configuration, the dye started to diffuse into the pipette, decreasing the fluorescence signal until a stable level was achieved ~10 min after the beginning of the intracellular dialysis. At this stage, the nuclear region, with significantly less fluorescence, became clearly visible (Figures 1, 3 and 4).

To measure simultaneously $[Ca^{2+}]_L$ and cytoplasmic Ca^{2+} concentration ($[Ca^{2+}]_i$), the intrapipette solution was supplemented with 0.05 mM of the high-affinity Ca^{2+} indicator Fluo-3K₅. Cell perfusion with Fluo-3K₅ did not significantly affect Mag-Fura-2 fluorescence. After 10 min of intracellular dialysis, Fluo-3 fluorescence also reached a steady-state level. Mag-Fura-2 and Fluo-3 signals were separated using their distinct excitation properties (340/380 nm for Mag-Fura-2 and 488 nm for Fluo-3). Fluo-3 is weakly excited at 350–380 nm; however, the level of Fluo-3 signal did not exceed 1–2% of the signals from Mag-Fura-2 measured at the same system settings.

Calibration of Mag-Fura-2 signals

The $[Ca^{2+}]_L$ values were calculated using the 340/380 nm ratio with the equation $[Ca^{2+}]_L = K^* (R - R_{min}) / (R_{max} - R)$. The R_{min} , R_{max} and K^* values were determined using exposure of neurons to 20 μ M ionomycin and four calibrating solutions with $[Ca^{2+}] < 10$ nM (10 mM EGTA); 100 μ M; 400 μ M and 10 mM; solutions were prepared as described previously (Tse *et al.*, 1994). Values for R_{min} , R_{max} and K^* were 0.27, 1.1 and 221 μ M, respectively.

Real-time video imaging

Fluorescence images were captured using an Olympus IX70 inverted microscope (40 \times UV objective) equipped with a charge-coupled device (CCD)-cooled intensified camera (Pentamax Gene IV, Roper Scientific). The specimen was illuminated alternately at 340, 380 and 488 nm by a monochromator (Polychrom IV, TILL Photonics, Germany) at a cycle frequency of 3–5 Hz. Control over the experiment, image storage and off-line analysis was performed by use of MetaFluor/MetaMorph software (Universal Imaging Corporation) running on a Windows 98 workstation.

Electrophysiology and solution exchange

Electrophysiological recordings were made by using an EPC-9 amplifier run by the PC-based PULS software (both from HEKA, Germany). The pipette resistance was 3–5 M Ω . Ca^{2+} currents were recorded in Na^+ -free solution to avoid contaminating Na^+ currents. Brief removal of Na^+ ions did not affect either $[Ca^{2+}]_i$ or $[Ca^{2+}]_L$. All solutions were applied using a fast local superfusion technique (Veselovsky *et al.*, 1996), which ensured complete exchange of the milieu surrounding the cell within 100 ms.

Solutions and reagents

The extracellular bathing solution contained: 135 mM NaCl, 3 mM KCl, 2 mM $CaCl_2$, 20 mM glucose, 20 mM HEPES–NaOH pH 7.4. The Ca^{2+} -free solution contained 5 mM EGTA with no $CaCl_2$ added. To obtain Na^+ -free solution, Na^+ ions were substituted by TEA–Cl and 0.1 μ M tetrodotoxin was added. The intracellular solution contained: 122 mM $CaCl_2$, 20 mM TEA–Cl, 3 mM Na_2ATP , 10 mM HEPES–CsOH pH 7.3. For $[Ca^{2+}]_i$ recordings, the intrapipette solution was supplemented with 0.05 mM Fluo-3 K₅. All reagents were purchased from Sigma and fluorescent probes were obtained from Molecular Probes.

Acknowledgements

This research was supported by a BBSRC research grant to A.V. (ref. 34/C12751) and by a Wellcome Trust collaborative grant to N.S. and A.V. (ref. 060095).

References

- Alford, S., Frenguelli, B.G., Schofield, J.G. and Collingridge, G.L. (1993) Characterization of Ca^{2+} signals induced in hippocampal CA1 neurones by the synaptic activation of NMDA receptors. *J. Physiol. (Lond.)*, **469**, 693–716.
- Alonso, M.T., Barrero, M.J., Michelena, P., Carnicero, E., Cuchillo, I., Garcia, A.G., Garcia-Sancho, J., Montero, M. and Alvarez, J. (1999) Ca^{2+} -induced Ca^{2+} release in chromaffin cells seen from inside the ER with targeted aequorin. *J. Cell Biol.*, **144**, 241–254.
- Berridge, M.J. (1993) Inositoltrisphosphate and calcium signalling. *Nature*, **361**, 315–325.
- Berridge, M.J. (1998) Neuronal calcium signaling. *Neuron*, **21**, 13–26.
- Bezprozvanny, I., Watras, J. and Ehrlich, B.E. (1991) Bell-shaped calcium-response curves of $Ins(1,4,5)P_3$ - and calcium-gated channels from endoplasmic reticulum of cerebellum. *Nature*, **351**, 751–754.
- Brorson, J.R., Bleakman, D., Gibbons, S.J. and Miller, R.J. (1991) The properties of intracellular calcium stores in cultured rat cerebellar neurons. *J. Neurosci.*, **11**, 4024–4043.
- Chatton, J.Y., Liu, H. and Stucki, J.W. (1995) Simultaneous measurements of Ca^{2+} in the intracellular stores and the cytosol of hepatocytes during hormone-induced Ca^{2+} oscillations. *FEBS Lett.*, **368**, 165–168.
- Emptage, N., Bliss, T.V.P. and Fine, A. (1999) Single synaptic events evoke NMDA receptor-mediated release of calcium from internal stores in hippocampal dendritic spines. *Neuron*, **22**, 115–124.
- Frenguelli, B.G., Irving, A.J. and Collingridge, G.L. (1996) Ca^{2+} stores and hippocampal synaptic plasticity. *Semin. Neurosci.*, **8**, 301–309.
- Friel, D.D. and Tsien, R.W. (1992) A caffeine- and ryanodine-sensitive Ca^{2+} store in bullfrog sympathetic neurones modulates effects of Ca^{2+} entry on $[Ca^{2+}]_i$. *J. Physiol. (Lond.)*, **450**, 217–246.
- Galione, A., Lee, H.C. and Busa, W.B. (1991) Ca^{2+} -induced Ca^{2+} release in sea urchin egg homogenates: modulation by cyclic ADP-ribose. *Science*, **253**, 1143–1146.
- Garaschuk, O., Yaari, Y. and Konnerth, A. (1997) Release and sequestration of calcium by ryanodine-sensitive stores in rat hippocampal neurones. *J. Physiol. (Lond.)*, **502**, 13–30.
- Golovina, V.A. and Blaustein, M.P. (1997) Spatially and functionally distinct Ca^{2+} stores in sarcoplasmic and endoplasmic reticulum. *Science*, **275**, 1643–1648.
- Golovina, V.A. and Blaustein, M.P. (2000) Unloading and refilling of two classes of spatially resolved endoplasmic reticulum Ca^{2+} stores in astrocytes. *Glia*, **31**, 15–28.
- Grynkiewicz, G., Poenie, M. and Tsien, R.Y. (1985) A new generation of Ca^{2+} indicators with greatly improved fluorescence properties. *J. Biol. Chem.*, **260**, 3440–3450.
- Han, S., Schiefer, A. and Isenberg, G. (1994) Ca^{2+} load of guinea-pig ventricular myocytes determines efficacy of brief Ca^{2+} currents as trigger for Ca^{2+} release. *J. Physiol. (Lond.)*, **480**, 411–421.
- Hardingham, G.E., Arnold, F.J. and Bading, H. (2001) Nuclear calcium signaling controls CREB-mediated gene expression triggered by synaptic activity. *Nature Neurosci.*, **4**, 261–267.
- Hernandez-Cruz, A., Escobar, A.L. and Jimenez, N. (1997) Ca^{2+} -induced Ca^{2+} release phenomena in mammalian sympathetic neurones are critically dependent on the rate of rise of trigger Ca^{2+} . *J. Gen. Physiol.*, **109**, 147–167.
- Hofer, A.M. and Schulz, I. (1996) Quantification of intraluminal free $[Ca]$ in the agonist-sensitive internal calcium store using compartmentalized fluorescent indicators: some considerations. *Cell Calcium*, **20**, 235–242.
- Hua, S.Y., Nohmi, M. and Kuba, K. (1993) Characteristics of Ca^{2+} release induced by Ca^{2+} influx in cultured bullfrog sympathetic neurones. *J. Physiol. (Lond.)*, **464**, 245–272.
- Hua, S.Y., Tokimasa, T., Takasawa, S., Furuya, Y., Nohmi, M., Okamoto, H. and Kuba, K. (1994) Cyclic ADP-ribose modulates Ca^{2+} release channels for activation by physiological Ca^{2+} entry in bullfrog sympathetic neurones. *Neuron*, **12**, 1073–1079.
- Kano, M., Garaschuk, O., Verkhratsky, A. and Konnerth, A. (1995) Ryanodine receptor-mediated intracellular calcium release in rat cerebellar Purkinje neurones. *J. Physiol. (Lond.)*, **487**, 1–16.
- Krizaj, D., Bao, J.X., Schmitz, Y., Witkovsky, P. and Copenhagen, D.R. (1999) Caffeine-sensitive calcium stores regulate synaptic transmission from retinal rod photoreceptors. *J. Neurosci.*, **19**, 7249–7261.
- Lipscombe, D., Madison, D.V., Poenie, M., Reuter, H., Tsien, R.W. and Tsien, R.Y. (1988) Imaging of cytosolic Ca^{2+} transients arising from Ca^{2+} stores and Ca^{2+} channels in sympathetic neurones. *Neuron*, **1**, 355–365.
- Llano, I., DiPollo, R. and Marty, A. (1994) Calcium-induced calcium release in cerebellar Purkinje neurones. *Neuron*, **12**, 663–673.
- Lukyanenko, V., Gyorke, I. and Gyorke, S. (1996) Regulation of calcium release by calcium inside the sarcoplasmic reticulum in ventricular myocytes. *Pflügers Arch.*, **432**, 1047–1054.
- Marrion, N.V. and Adams, P.R. (1992) Release of intracellular calcium and modulation of membrane currents by caffeine in bullfrog sympathetic neurones. *J. Physiol. (Lond.)*, **445**, 515–535.
- Maruyama, Y., Inooka, G., Li, Y.X., Miyashita, Y. and Kasai, H. (1993) Agonist-induced localized Ca^{2+} spikes directly triggering exocytotic secretion in exocrine pancreas. *EMBO J.*, **12**, 3017–3022.
- Mogami, H., Tepikin, A.V. and Petersen, O.H. (1998) Termination of cytosolic Ca^{2+} signals: Ca^{2+} reuptake into intracellular stores is regulated by the free Ca^{2+} concentration in the store lumen. *EMBO J.*, **17**, 435–442.
- Niggli, E. (1999) Localized intracellular calcium signaling in muscle: calcium sparks and calcium quarks. *Annu. Rev. Physiol.*, **61**, 311–335.
- Park, M.K., Tepikin, A.V. and Petersen, O.H. (1999) The relationship between acetylcholine-evoked Ca^{2+} -dependent current and the Ca^{2+}

- concentrations in the cytosol and the lumen of the endoplasmic reticulum in pancreatic acinar cells. *Pflügers Arch.*, **438**, 760–765.
- Park,M.K., Petersen,O.H. and Tepikin,A.V. (2000) The endoplasmic reticulum as one continuous Ca^{2+} pool: visualization of rapid Ca^{2+} movements and equilibration. *EMBO J.*, **19**, 5729–5739.
- Paschen,W. (2001) Dependence of vital cell function on endoplasmic reticulum calcium levels: implications for the mechanisms underlying neuronal cell injury in different pathological states. *Cell Calcium*, **29**, 1–11.
- Petersen,O.H., Petersen,C.C. and Kasai,H. (1994) Calcium and hormone action. *Annu. Rev. Physiol.*, **56**, 297–319.
- Petersen,O.H., Tepikin,A. and Park,M.K. (2001) The endoplasmic reticulum: one continuous or several separate Ca^{2+} stores? *Trends Neurosci.*, **24**, 271–276.
- Rose,C.R. and Konnerth,A. (2001) Stores not just for storage. Intracellular calcium release and synaptic plasticity. *Neuron*, **31**, 519–522.
- Shmigol,A., Verkhratsky,A. and Isenberg,G. (1995) Calcium-induced calcium release in rat sensory neurones. *J. Physiol. (Lond.)*, **489**, 627–636.
- Shmigol,A., Svichar,N., Kostyuk,P. and Verkhratsky,A. (1996) Gradual caffeine-induced Ca^{2+} release in mouse dorsal root ganglion neurons is controlled by cytoplasmic and luminal Ca^{2+} . *Neuroscience*, **73**, 1061–1067.
- Sitsapesan,R. and Williams,A.J. (1990) Mechanisms of caffeine activation of single calcium-release channels of sheep cardiac sarcoplasmic reticulum. *J. Physiol. (Lond.)*, **423**, 425–439.
- Thayer,S.A., Hirning,L.D. and Miller,R.J. (1988) The role of caffeine-sensitive calcium stores in the regulation of the intracellular free calcium concentration in rat sympathetic neurons *in vitro*. *Mol. Pharmacol.*, **34**, 664–673.
- Thomas,D., Tovey,S.C., Collins,T.J., Bootman,M.D., Berridge,M.J. and Lipp,P. (2000) A comparison of fluorescent Ca^{2+} indicator properties and their use in measuring elementary and global Ca^{2+} signals. *Cell Calcium*, **28**, 213–223.
- Thorn,P., Lawrie,A.M., Smith,P.M., Gallacher,D.V. and Petersen,O.H. (1993) Local and global cytosolic Ca^{2+} oscillations in exocrine cells evoked by agonists and inositol trisphosphate. *Cell*, **74**, 661–668.
- Tse,F.W., Tse,A. and Hille,B. (1994) Cyclic Ca^{2+} changes in intracellular stores of gonadotropes during gonadotropin-releasing hormone-stimulated Ca^{2+} oscillations. *Proc. Natl Acad. Sci. USA*, **91**, 9750–9754.
- Usachev,Y.M. and Thayer,S.A. (1997) All-or-none Ca^{2+} release from intracellular stores triggered by Ca^{2+} influx through voltage-gated Ca^{2+} channels in rat sensory neurons. *J. Neurosci.*, **17**, 7404–7414.
- Usachev,Y., Shmigol,A., Pronchuk,N., Kostyuk,P. and Verkhratsky,A. (1993) Caffeine-induced calcium release from internal stores in cultured rat sensory neurons. *Neuroscience*, **57**, 845–859.
- Verkhratsky,A. and Petersen,O.H. (1998) Neuronal calcium stores. *Cell Calcium*, **24**, 333–343.
- Verkhratsky,A. and Shmigol,A. (1996) Calcium-induced calcium release in neurones. *Cell Calcium*, **19**, 1–14.
- Veselovsky,N.S., Engert,F. and Lux,H.D. (1996) Fast local superfusion technique. *Pflügers Arch.*, **432**, 351–354.
- Zucker,R.S. (1996) Exocytosis: a molecular and physiological perspective. *Neuron*, **17**, 1049–1055.

Received November 26, 2001; revised and accepted December 17, 2001